

Relationship between the time-domain Kohlrausch-Williams-Watts and frequency-domain Havriliak-Negami relaxation functions

F. Alvarez, A. Alegría, and J. Colmenero

*Departamento de Física de Materiales, Facultad de Química,
Apartado 1072, 20080 San Sebastián, Spain*

(Received 24 April 1991)

The Kohlrausch-Williams-Watts (KWW) and the Havriliak-Negami (HN) relaxation functions have been widely used to describe the relaxation behavior of glass-forming liquids and complex systems. While the HN relaxation function is a frequency function, the natural domain of the KWW relaxation function is time (although it has also been used with frequency-domain spectroscopies). A relationship among the parameters of the two models is suggested by the fact that both models yield an accurate description of real data. Nevertheless, this relationship cannot be an analytical one, since it is known that the HN and the KWW relaxation functions are not exactly Fourier transforms of each other. In order to find out the nature of this relationship, a method which makes use of a distribution of relaxation times is proposed here. Numerical simulations following the KWW model have been assumed to describe the relaxation behavior in time; likewise, the HN description was assumed to be valid for the frequency domain. From this work, a connection among the parameters of both models is obtained, which is expected to be valid for those experimental data that can be described by either the KWW or the HN model. This is the case for most, if not all, measurements on the dynamics in complex systems and glass-forming liquids that frequently appear in the literature. The proposed procedure has been tested by using dielectric-spectroscopy measurements, both in frequency and time domains to study the α relaxation in a glass-forming polymeric system, poly(hydroxy ether of bisphenol-*A*).

I. INTRODUCTION

A theoretical description of the slow relaxation in complex condensed systems is still a topic of active research despite the great effort made in recent years. In the time domain there seems to be a universal function that slow relaxations obey. This is the well known Kohlrausch-Williams-Watts (KWW) function, which is also currently called a "stretched exponential,"

$$\phi(t) = \exp \left[- \left(\frac{t}{\tau_{\text{ww}}} \right)^\beta \right],$$

where τ_{ww} is a characteristic relaxation time and β is a parameter ranging between 0 and 1. This function was introduced in 1863 to describe mechanical creep in glassy fibers¹ and was later used by Williams and Watts² in 1970 to describe dielectric relaxation in polymers. Lately, this function has been used to fit miscellaneous experimental data, including data from mechanical, NMR, dielectric, enthalpic, volumetric, dynamic light scattering, magnetic relaxation, quasielastic neutron scattering, kinetics reactions, etc. (for example, the general Refs. 3–5). Nowadays, it is also well known that the KWW law can be derived from several different physical or mathematical models ranging from models based on distributions of relaxation times to complex correlated processes (these models have been summarized in several references; see, for example, Refs. 6 and 7).

In order to analyze KWW in the frequency domain, a Fourier transform is needed. However, it is well known that there is no analytical expression for the Fourier

transform of the KWW function. Several numerical methods have been used to Fourier transform the KWW function and to interpret relaxation data from spectroscopies in the frequency domain. However, it is also well known that computation of Fourier transform poses numerical problems originating from cutoff effects which yield unwanted oscillations, especially when treating real data.

On the other hand, the experimental relaxation behavior of glass-forming liquids has usually been described since 1967 through an empirical relaxation function introduced by Havriliak and Negami (HN):⁸

$$\phi_{\text{HN}}^*(\omega) = \frac{1}{[1 + (i\omega\tau_H)^\alpha]^\gamma},$$

where τ_H is a characteristic relaxation time and α and γ are parameters ranging between 0 and 1, namely, this relaxation function has been widely used to describe data from dielectric spectroscopies.^{9–13} Recently, this kind of relaxation function has also been used by us to analyze nuclear magnetic relaxation measurements^{14–16} as well as quasielastic neutron scattering data^{15–17} in glass-forming polymeric systems.

These results suggest that there should be a connection among the parameters of the KWW and the HN functional forms. The finding of the mathematical expression of these relationships was the main purpose of this work. To do this, and in order to avoid problems associated to the numerical Fourier transform, we have developed a method based on the introduction of a distribution of relaxation times, which, at least in a first consideration,

should be interpreted only as a mathematical tool. There is no need for KWW or HN functions to be used here, because the method can be equally valid if performed on any relaxation function or even on real data.

The results obtained have been tested by using data from dielectric spectroscopy, both in time and in frequency domains, corresponding to α relaxation in a glass-forming polymer: poly(hydroxy ether of bisphenol-A) (PH).

II. THEORETICAL BACKGROUND

A. The KWW function

As it has been mentioned above, the analytical expression of this function is given by

$$\phi(t) = \exp[-(t/\tau_{\text{WW}})^\beta], \quad (1)$$

where $0 < \beta \leq 1$. Equation (1) can be correctly described, from the mathematical point of view, as a superposition of uncoupled Debye processes in the following way:

$$\exp[-(t/\tau_{\text{WW}})^\beta] = \int_0^\infty \exp(-t/\tau) \rho(\tau) d\tau, \quad (2)$$

where $\rho(\tau)$ is the distribution of Debye relaxation times. In general it is not clear what $\rho(\tau)$ physically means. But, in any case, we can consider $\rho(\tau)$ on Eq. (2) as a mathematical tool. Due to the wide time range covered, it is usually preferred to define the distribution in logarithm of time instead of taking the linear time scale:

$$\exp[-(t/\tau_{\text{WW}})^\beta] = \int_{-\infty}^\infty \exp(-t/\tau) L(\ln\tau) d \ln\tau. \quad (3)$$

The connection between both distributions is given by $L(\ln\tau) = \tau\rho(\tau)$.

An average relaxation time is usually defined in terms of the γ function as

$$\langle \tau \rangle = \frac{\tau_{\text{WW}}}{\beta} \Gamma\left[\frac{1}{\beta}\right], \quad (4)$$

which corresponds to the integrated area of the KWW function. Higher moments are given by

$$\langle \tau^n \rangle = \frac{\tau_{\text{WW}}^n}{\beta} \frac{\Gamma(n/\beta)}{\Gamma(n)}, \quad (5)$$

which comes out from the definition of the moments of the distribution:

$$\langle \tau^n \rangle = \int_0^\infty \tau^n \rho(\tau) d\tau = \frac{1}{\Gamma(n)} \int_0^\infty t^{n-1} \phi(t) dt. \quad (6)$$

Likewise, an average frequency (which is different to $1/\langle \tau \rangle$) can be defined

$$\langle \omega^n \rangle = \int_0^\infty \frac{1}{\tau^n} \rho(\tau) d\tau = (-1)^n \frac{d^n \phi(0)}{dt^n}. \quad (7)$$

But the derivative of the KWW function is given by

$$\frac{d\phi(t)}{dt} = -\frac{\beta}{\tau_{\text{WW}}} \left[\frac{t}{\tau_{\text{WW}}} \right]^{\beta-1} \phi(t), \quad (8)$$

and it diverges at $t=0$. Therefore, average relaxation fre-

quencies cannot be defined. That the derivative diverges as $t \rightarrow 0$ could preclude a physical interpretation of the KWW function.

The $L(\ln\tau)$ corresponding to the KWW function can be written in the following way:

$$L(\ln\tau) = \frac{1}{\pi x} \int_0^\infty \exp(-xu) \exp[-u^\beta \cos(\pi\beta)] \times \sin[u^\beta \sin(\pi\beta)] du, \quad (9)$$

where $x = \tau/\tau_{\text{WW}}$. This integral has a closed analytical form for $\beta=0.5$:

$$L(\ln\tau) = \frac{1}{2} \pi^{-1/2} x^{-3/2} e^{-1/4x}. \quad (10)$$

For different values of the β parameter it is necessary to evaluate the previous integral or alternatively the following series form:

$$L(\ln\tau) = -\frac{1}{\pi} \sum_{k=0}^{\infty} \frac{(-1)^k}{k!} \sin(\pi\beta k) \frac{\Gamma(\beta k + 1)}{x^{\beta k + 1}}. \quad (11)$$

Computation of the distribution function by calculating the preceding integral or the series form is cumbersome because there are terms which can take values many orders larger than the final result of the summation. Thus, a high precision is required for accuracy that is, many significant figures must be retained in the computation. Furthermore, algorithms which yield values for trigonometric functions can fail when their arguments are high, and this can become another source of error.

On the other hand, Provencher's CONTIN program¹⁸ has proven to be a reliable tool to obtain $\rho(\tau)$. As it will be mentioned further, we have altered some of the variables in order to get $L(\ln\tau)$ directly spaced in logarithm. Our procedure seems to be somewhat similar to the one reported in Ref. 19, but, while this one only gives the moments of $\langle \ln\tau \rangle$ (which is not equal to $\ln\langle \tau \rangle$ for nonsymmetric distributions like the KWW one), ours yields $\langle \tau \rangle$ directly.

B. The HN function

By using several frequency-domain spectroscopies, it was empirically found that the following expression for the relaxation functions was a good fit to the data:

$$\chi^*(\omega) = \chi_\infty + (\chi_s - \chi_\infty) \frac{1}{[1 + (i\omega\tau_H)^\alpha]^\gamma}, \quad (12)$$

where χ_∞ represents the asymptotical value of the susceptibility at high frequencies, and χ_s is the value of the opposite limit. This expression is known as the Havriliak-Negami (HN) function and has the following associated distribution of relaxation times:

$$g(\tau) = \frac{1}{\pi} \frac{(\tau/\tau_H)^{\alpha\gamma} \sin(\gamma\theta)}{[(\tau/\tau_H)^{2\alpha} + 2(\tau/\tau_H)^\alpha \cos(\alpha\pi) + 1]^{\gamma/2}}, \quad (13)$$

where θ is

$$\theta = \arctan \left| \frac{\sin(\gamma\pi)}{(\tau/\tau_H)^\alpha + \cos(\alpha\pi)} \right|, \quad (14)$$

and, consequently, the expressions for the real and imaginary parts of χ^* are

$$\chi' = \chi_\infty + (\chi_s - \chi_\infty) \frac{\cos(\gamma\phi)}{\{1 + 2(\omega\tau_H)^\alpha \sin[\pi/2(1-\alpha)] + (\omega\tau_H)^{2\alpha}\}^{\gamma/2}}, \quad (15)$$

$$\chi'' = (\chi_s - \chi_\infty) \frac{\sin(\gamma\phi)}{\{1 + 2(\omega\tau_H)^\alpha \sin[\pi/2(1-\alpha)] + (\omega\tau_H)^{2\alpha}\}^{\gamma/2}}, \quad (16)$$

with

$$\phi = \arctan \left[\frac{(\omega\tau_H)^\alpha \cos[\pi/2(1-\alpha)]}{1 + (\omega\tau_H)^\alpha \sin[\pi/2(1-\alpha)]} \right]. \quad (17)$$

From these expressions it can be seen that the maximum of the imaginary part, χ'' , is given by the following equation:

$$\omega\tau_H = \left[\tan \left[\frac{\pi}{2(\gamma+1)} \right] \right]^{1/\alpha}. \quad (18)$$

Through the Cole-Cole diagram (representation of χ'' versus $\chi' - \chi_\infty$) the values of α and γ can be deduced from the high and low frequency behaviors of the susceptibility. This is so because, as $\omega \rightarrow \infty$,

$$\frac{\chi^* - \chi_\infty}{\chi_s - \chi_\infty} \sim (i\omega\tau_H)^{-\alpha\gamma} = (\omega\tau_H)^{-\alpha\gamma} [\cos(\alpha\gamma\pi/2) - i \sin(\alpha\gamma\pi/2)], \quad (19)$$

$$\tan(\alpha\gamma\pi/2) = \frac{\chi''(\omega \rightarrow \infty)}{\chi'(\omega \rightarrow \infty) - \chi_\infty}, \quad (20)$$

whereas, as $\omega \rightarrow 0$,

$$\frac{\chi^* - \chi_\infty}{\chi_s - \chi_\infty} \sim 1 - \gamma(i\omega\tau_H)^\alpha = 1 - \gamma(\omega\tau_H)^\alpha [\cos(\alpha\pi/2) + i \sin(\alpha\pi/2)], \quad (21)$$

$$\tan(\alpha\pi/2) = \frac{\chi''(\omega \rightarrow 0)}{\chi_s - \chi'(\omega \rightarrow 0)}. \quad (22)$$

Thus, from these asymptotical behaviors of χ' and χ'' it can be seen that, at very high frequencies $(\chi' - \chi_\infty) \propto \chi'' \propto \omega^{-\alpha\gamma}$, whereas low frequencies give $(\chi_s - \chi') \propto \chi'' \propto \omega^\alpha$. These behaviors are both experimentally observed in real and imaginary parts of $\chi^*(\omega)$ in almost all materials, and it induced several authors to think about relaxation in solids as a many-body problem.²⁰⁻²² This interpretation seems to be a realistic alternative to the superposition of elementary Debye processes.

III. COMPUTATIONAL METHOD

A program developed by Provencher called CONTIN (Ref. 18) was utilized to get the distribution of relaxation times out of the KWW function by means of an inverse Laplace Transform. Likewise, to obtain the distribution from the HN function, an algorithm proposed by Imanishi, Adachi, and Kotaka²³ was used. Once we get this distribution we can easily perform an integration to calculate the appropriate relaxation function, either in time or in frequency domain. Both programs can be used with real data.

Thus, if we enter a KWW function with a certain β parameter in the CONTIN program, we can obtain the corresponding distribution, which leads to the frequency relaxation function. The fitting of this function to the HN expression will yield the values of the HN parameters which correspond to the previously chosen β parameter. Moreover, if we use the algorithm proposed in Ref. 23 with this frequency function we should recover the distribution of relaxation times, and, when integrating, the initial KWW parameter.

This method is explicitly shown here for the arbitrarily chosen $\beta=0.55$ parameter.

First of all, a KWW function is numerically generated and introduced in the CONTIN program to obtain the distribution of relaxation times. Both are shown in Fig. 1. Once we have the $g(\ln\tau)$, we can perform the following integration to obtain the loss peak:

$$\frac{\chi''(\omega)}{\chi_s - \chi_\infty} = \int_{-\infty}^{\infty} \frac{\omega\tau}{1 + \omega^2\tau^2} g(\ln\tau) d(\ln\tau). \quad (23)$$

The result and its fits to the HN function with two different sets of α and γ parameters are given in Fig. 2.

These fits are obtained through a multiparameter minimization subroutine based on the downhill simplex method.²⁴ The discontinuous line fit corresponds to the case in which all available points of the computed loss peak have been used to perform the minimization. For the continuous line fit, a constricted minimization has been performed by taking just the central points. The fact that there is no set of HN parameters that exactly matches the computed susceptibility loss peak was to be expected and can be understood on the grounds that HN and KWW functions are not the exact analytical Fourier

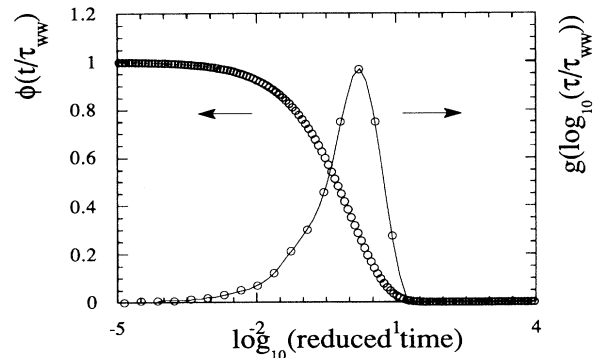


FIG. 1. Generated Kohlrausch-Williams-Watts function, $\phi(t)$, of $\beta=0.55$ and its associated distribution of relaxation times $g(\log_{10}\tau)$ obtained by ILT.

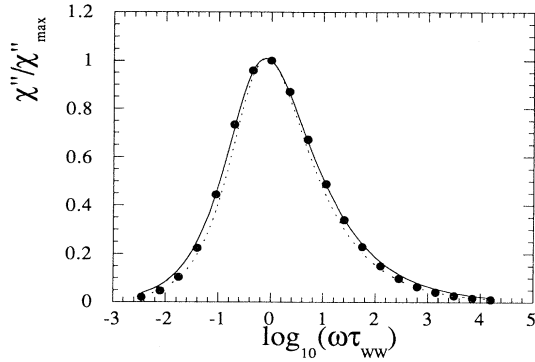


FIG. 2. Computed loss peak from $g(\log_{10}\tau)$ and Eq. (24) and its fit with two sets of HN parameters: The solid line is for $\alpha=0.818, \gamma=0.561$, and the dotted one for $\alpha=0.875, \gamma=0.568$.

transforms of one another. Although the standard deviation is less for the second set of parameters (those which match better the low and high frequency regions), we should choose the criterion of selecting the first set as the one which corresponds to the β value of 0.55. This is so because it is this set which best describes the central part of the peak. The reason to do this is based on the fact

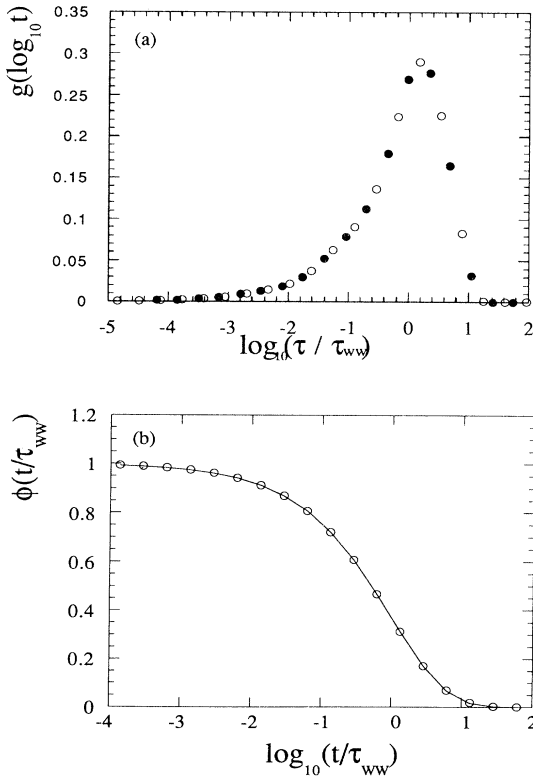


FIG. 3. (a) Comparison between the original $g(\log_{10}\tau)$ and the one obtained from $\chi''(\omega)$ by the algorithm of Ref. 18. (b) Computed time relaxation function with the $g(\log_{10}\tau)$ obtained from $\chi''(\omega)$ and its fit to the Williams-Watts function ($\beta=0.551, \tau=\tau_{ww}1.009$).

that, in real experimental measurements, the most reliable region is precisely the zone around the peak, for the tails can be distorted by other nearby processes. Besides, also experimental devices might not have a wide enough available frequency range to reach the base line.

So far we have suggested how to obtain the α and γ parameters for a HN function starting from a chosen β value for the KWW function. Now, if we want to proceed in the opposite way, namely, from the HN parameters to the KWW parameter, we take the Adachi and Kotaka algorithm.²⁵ This algorithm is based upon an iterative calculation, which consists in modifying the distribution of relaxation times by adding to it an amount proportional to the difference between the original susceptibility loss peak, and the calculated loss peak from the distribution of relaxation times corresponding to the prior iteration. This difference is evaluated at each point, which means that to correct the $g(\ln\tau)$ in τ we need to estimate the difference in $\omega=1/\tau$.

If we want to test the consistency of this theory we should apply it to the previously shown loss peak and get back to a β value of 0.55. Thus, we have taken the susceptibility loss peak calculated from the output distribution and we have operated on it with the Adachi and Kotaka algorithm to see whether we recover the original distribution of relaxation times. The result is shown in Fig.

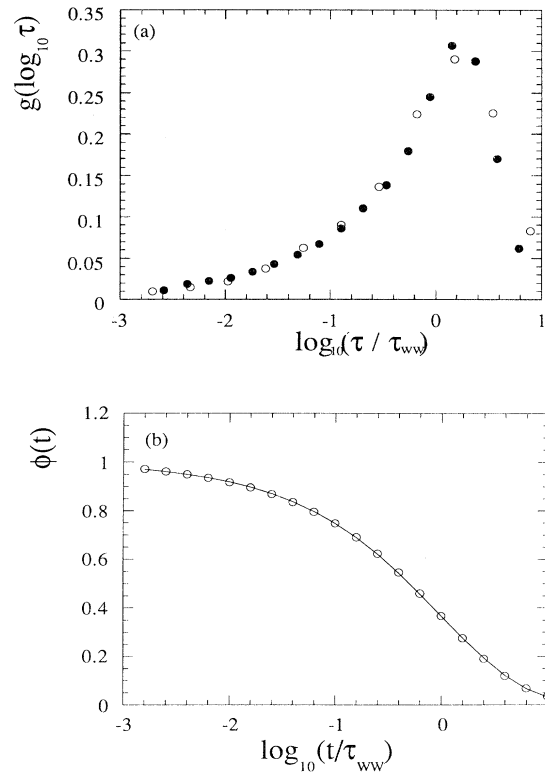


FIG. 4. (a) Comparison between the original $g(\log_{10}\tau)$ and the one obtained from the fit of $\chi''(\omega)$ to a Havriliak-Negami function. (b) Computed time relaxation function with the $g(\log_{10}\tau)$ obtained from the HN fit of $\chi''(\omega)$ and its fit to the Williams-Watts function ($\beta=0.54, \tau=\tau_{ww}$).

3(a), where the open symbols correspond to the CONTIN distribution and the solid symbols are those obtained from the Adachi-Kotaka algorithm. As we can see, the agreement is excellent. Now we can perform the following integration to obtain the time-domain relaxation function:

$$\phi(t) = \int_{-\infty}^{\infty} \exp(-t/\tau) L(\ln\tau) d \ln\tau. \quad (24)$$

By fitting the so obtained $\phi(t)$ to the KWW expression, we get the result shown in Fig. 3(b) which shows that the original values for β and τ are recovered. To be more accurate, we should recall that the HN expression did not exactly match the loss peak obtained from the CONTIN distribution, so we should generate the loss peak of a HN expression corresponding to the previously obtained best fit values and then introduce it in the Adachi-Kotaka algorithm. In Figs. 4(a) and 4(b) we show these results, where the open symbols denote, as before, the CONTIN distribution and the solid ones are those obtained from the HN loss peak with the chosen values. It should be noted here that the existing analytical expressions for the distributions of the KWW and the HN functions are markedly different (the HN analytical distribution shows a sharp cutoff in the long times side, while the KWW one is close to the CONTIN distribution), whereas the ones shown here are similar. This fact supports our decision of rejecting these analytical expressions.

Figure 4(b), which shows that the time-domain relaxation function calculated from a HN simulation can be fitted (for these parameters and this interval) with a KWW function, can be understood as a test of the reliability of the method, and allows us to state that both, a KWW function with a β value of 0.55 and a HN function with $\alpha=0.82$, $\gamma=0.56$, describe the same relaxation functions in time and frequency.

Table I lists the results obtained from following the

TABLE I. Values of the HN parameters corresponding to the fitting of the frequency-domain response function deduced for the stretched exponential with the chosen β parameters.

β	α	γ	τ_H/τ_{ww}
0.10	0.2190	0.3182	310.46
0.15	0.3115	0.3705	32.456
0.20	0.3944	0.3968	14.863
0.25	0.5164	0.3706	10.000
0.30	0.5442	0.4667	5.0119
0.35	0.6741	0.4074	5.3827
0.40	0.7175	0.4487	3.9446
0.45	0.7976	0.4439	3.6224
0.50	0.8091	0.5105	2.9174
0.55	0.8180	0.5610	2.3659
0.60	0.8801	0.5981	2.0137
0.65	0.9334	0.6193	1.9364
0.70	0.9406	0.6954	1.6711
0.75	0.9554	0.7420	1.5668
0.80	0.9699	0.7780	1.5031
0.85	0.9870	0.8417	1.4421
0.90	0.9832	0.8688	1.1858
0.95	0.9930	0.9314	1.0666

above described procedure for different β values. These results have been plotted in Fig. 5(a).

The fact that a KWW function can be fitted with a HN expression does not mean that the inverse is always true. For the values that appear in Table I, the equivalence can be stated, as we proved for $\alpha=0.818$, $\gamma=0.561$, but it will not be the case, in general, for arbitrary α, γ . This can be understood from the fact that the HN function can be considered as a more versatile function than the KWW one, in the sense that it has one more parameter. However, a possible relationship among α , γ , and β is hinted by the results on Table I. This originates from the fact that $\alpha\gamma \approx \beta$, as can be seen in Fig. 5(b). This condition is already suggested from results on Refs. 11 and 12. Actually, the following analytical relations can be derived from the data shown in Table I:

$$\ln \left[\frac{\tau_H}{\tau_{\text{ww}}} \right] = 2.6(1-\beta)^{0.5} \exp(-3\beta) \quad (25)$$

for the characteristic times and

$$\alpha\gamma = \beta^{1.23} \quad (26)$$

for the shape parameters, and allow a direct way of transformation from the HN parameters into the KWW ones.

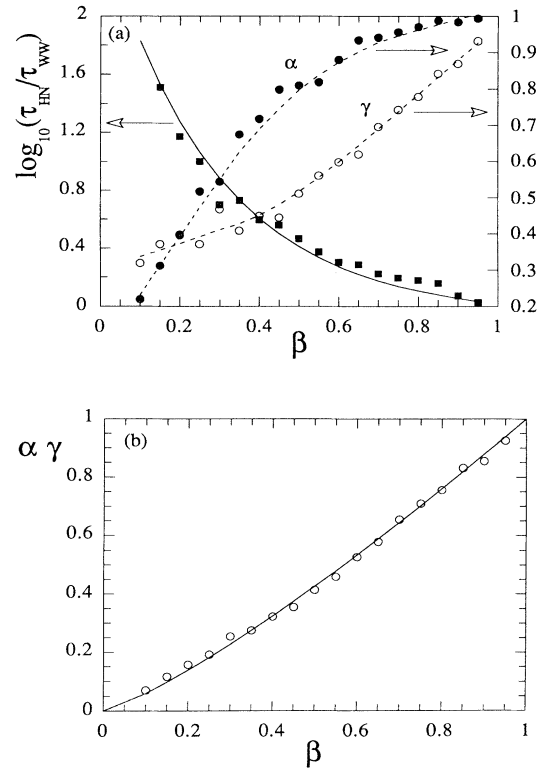


FIG. 5. (a) Values of the HN fitting parameters as functions of the corresponding β values. The solid line is from Eq. (25). The dotted ones are guides for the eye. (b) Plot of the product $\alpha\gamma$ as a function of the corresponding β values. The solid line stands for Eq. (26).

IV. TEST WITH REAL DATA

The reliability of the method was tested with real dielectric measurements performed around the α relaxation of poly(hydroxy ether of bisphenol-*A*) (PH). For this purpose, two spectroscopic techniques were used: one acting in time domain, namely, the transient currents method,^{25,26} and the other in frequency domain, the dielectric relaxation spectroscopy (DRS).

The glass transition temperature of the PH used, as measured by Differential Scanning Calorimetry and derived from the inflection point of the scan corresponding at 10°/min heating rate, was 370 K.

For the transient current method, a constant dc voltage of 400 V was applied during an hour to a parallel-plate capacitor 1 mm thick and 25 mm in diameter. When the field was removed, the isothermal depolarization current was measured as a function of time with a Keithley 642 electrometer. This procedure was used at the temperatures of 371 and 373 K. This was so because it is in this temperature range that the equilibrium polarization was attained, allowing an available time range of the depolarization current to be measured with our experimental setup.

The dielectric measurements in the frequency domain

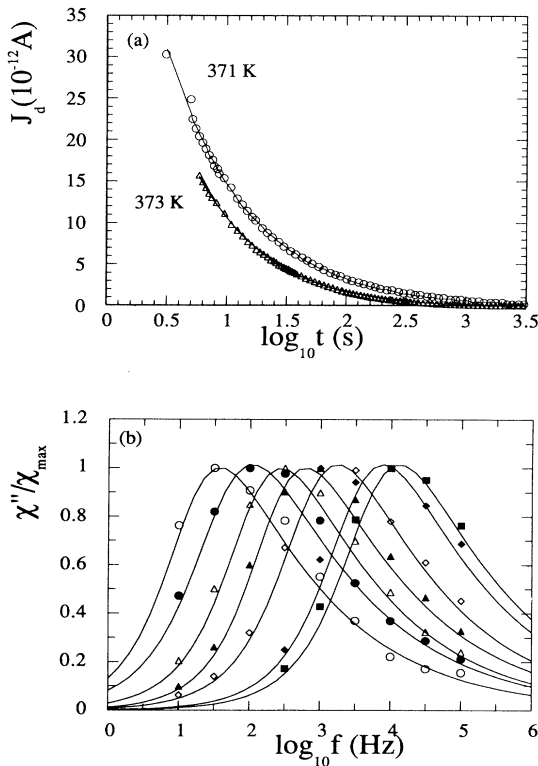


FIG. 6. (a) Fitting of the depolarized current to Eq. (7) at $T=371$ K ($\beta=0.391$, $\log_{10}\tau=3.84$), and $T=373$ K ($\beta=0.395$, $\log_{10}\tau=2.28$). (b) Isothermal loss peak curves and their fits to the HN expression at $T=385$ (○), 387 (●), 389 (△), 391 (▲), 393 (◇), 397 (◆), and 399 K (■).

covered the range from the audio-frequency up to the radio-frequency region. The measurement system uses a lock-in amplifier EG&G PAR 5208 with an internal oscillator, allowing a frequency range between 10 Hz and 100 kHz to be covered. The stray capacitance of the cell was reduced to 10^{-14} F. The sample was held between two condenser aluminum plates that were kept at a fixed distance. The capacitance of the sample cell was of the order of 10^{-11} F. A standard 10 pF air capacitor was used as reference in order to minimize errors in dielectric loss measurements, so the experimental limit for the loss factor value was about 10^{-4} . The measurements were performed doing frequency scans at isothermal conditions at temperatures between 380 and 400 K. Then, the real and imaginary parts of the dielectric susceptibility ($\chi^*=\chi'-i\chi''$) were obtained as a function of frequency and temperature. In order to extend the frequency range available to higher frequencies, a HP 4342A Q-meter (22 kHz–70 MHz) was used. In this case the measurements were performed at constant frequencies, and the loss factor was measured as a function of the temperature, this being the rate of the temperature scans 0.2 K/min.

Figure 6(a) shows the fit of the depolarization transient currents obtained at $T=371$ and 373 K with Eq. (8). As can be seen, the dynamics of the α relaxation of PH experimentally observed in the time domain is described very well by the KWW law.

Figure 6(b) shows the isothermal dielectric loss curves and their fit with the HN expression. The agreement between the experimental data and the fitting curves [Eq. (16)] is also very good. By means of the relationships be-

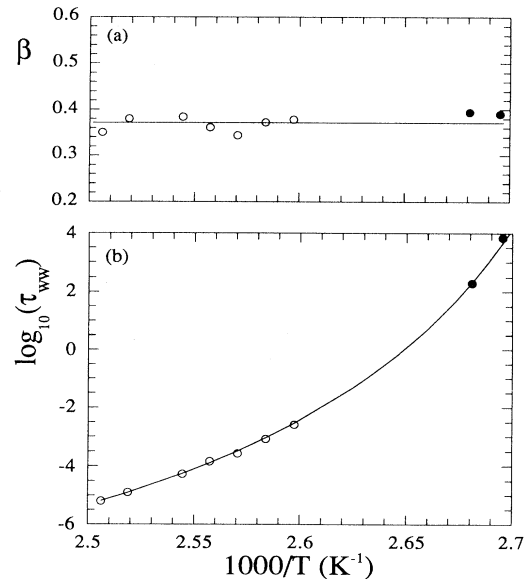


FIG. 7. (a) Comparison between the β values measured (solid points) from time-domain response and those obtained following the method presented in this work from frequency-domain response (open symbols). (b) Fitting of the τ_{WW} from transient current measurements (solid points) in the Vogel-Fulcher law taken from frequency dielectric measurements.

tween the HN and the KWW parameters obtained above [Eqs. (26) and (27)], we have calculated both the τ_{WW} and β parameter corresponding to the dynamics of the α relaxation, as observed in the frequency domain at each measured temperature. The results for the KWW parameters have been plotted versus temperature in Fig. 7.

Figure 7(a) shows that the β values obtained from both frequency and time domains are not dependent on temperature for this polymer. Moreover, the fact that this parameter is not dependent on the experimental domain used is an additional proof of the reliability of the method proposed in this work. However, as Fig. 7(b) shows, the values of the characteristic relaxation time τ_{WW} are very dependent on temperature as it is commonly found for the α relaxation of amorphous polymers like PH.²⁶ In order to obtain the law describing such temperature dependence, we have fitted the behavior of the temperature corresponding to the maxima of loss peaks obtained by means of temperature scans at a fixed frequency in the range 10–10⁷ Hz. Then the reciprocal of the frequency at the maximum loss has been fitted by means of a Vogel-Fulcher (VF) law:^{27,28}

$$\frac{1}{f} = 5 \times 10^{-11} \exp \left[\frac{749 \text{ K}}{T - 350 \text{ K}} \right] \text{ Hz}^{-1}. \quad (27)$$

The solid line in Fig. 7(b) displays the VF curve corresponding to Eq. (28) shifted in the time scale to match the τ_{WW} values deduced from the frequency-domain measurements. As it is clearly shown, the extrapolation of the behavior obtained in frequency domain fits perfectly to the one obtained in time domain, which proves again the reliability of the method here proposed.

V. CONCLUSIONS

The equivalence between the KWW and the HN functions has been studied here by using an alternative method to the analytical Fourier transformation. The validity of the relationships derived above has been proven to work for the α relaxation of PH. We expect this validity to hold for any system whose behavior is describable by either the KWW or HN relaxation functions.

ACKNOWLEDGMENTS

This work was supported in part by UPV the Universidad del País Vasco—Euskal Herriko Unibertsitatea EHU Project: UPV89 COD.206.215-0029/89 and by CICYT Project: MEC MAT89-0186. We also thank Gipuzkoako Foru Aldundia for partial financial support.

- ¹F. Kohlrausch, Pogg. Ann. Phys. **119**, 352 (1863).
- ²G. Williams and D. C. Watts, Trans. Faraday Soc. **66**, 80 (1970).
- ³*Non-Debye Relaxation in Condensed Matter*, edited by T. V. Ramakrishnan and M. Raj Lakshmi (World Scientific, Singapore, 1987).
- ⁴*Polymer Motion in Dense Systems*, edited by D. Richter and T. Springer (Springer-Verlag, Berlin, 1988).
- ⁵*Dynamics of Disordered Materials*, edited by D. Richter, A. J. Dianoux, W. Petry, and J. Teixeira (Springer-Verlag, Berlin, 1989).
- ⁶A. K. Rajagopal and K. L. Ngai, in *Relaxations in Complex Systems*, edited by K. L. Ngai and G. B. Wright (Office of Naval Research, Washington, D.C., 1986), p. 275. Available from National Technical Information Service, U.S. Department of Commerce, 5285 Port Royal Road, Springfield, VA 22161.
- ⁷M. F. Shlesinger and J. Klafter, in *Fractal in Physics*, edited by L. P. Pietronero and E. Tosatti (North-Holland, Amsterdam, 1986), p. 393.
- ⁸S. Havriliak and S. Negami, Polymer **8**, 161 (1967).
- ⁹A. Alegría, J. Colmenero, J. J. del Val, and J. M. Barandiarán, Polymer **26**, 913 (1985).
- ¹⁰Shioya, Mashimo, J. Chem. Phys. **87**, 3173 (1987).
- ¹¹D. Boese, B. Momper, G. Meier, F. Kremer, J.-U. Hagenah, and E. W. Fischer, Macromolecules **22**, 4416 (1989).
- ¹²D. Boese, F. Kremer, and F. J. Fetters, Macromolecules **23**, 829 (1990).
- ¹³G. Meier, B. Gerharz, D. Boese, and E. W. Fischer, J. Chem. Phys. **94**, 3050 (1991).
- ¹⁴J. M. Alberdi, F. Alvarez, A. Alegría, and J. Colmenero, in *Basic Features of the Glassy State*, edited by J. Colmenero and A. Alegría (World Scientific, Singapore, 1990), p. 252.
- ¹⁵J. Colmenero, J. Non-Cryst. Solids **131-133**, 860 (1991).
- ¹⁶J. Colmenero, A. Alegría, J. M. Alberdi, and B. Frick, J. Non-Cryst. Solids **131-133**, 949 (1991).
- ¹⁷J. Colmenero, A. Alegría, J. M. Alberdi, F. Alvarez, and B. Frick, Phys. Rev. B **44**, 7321 (1991).
- ¹⁸S. W. Provencher, Comput. Phys. Commun. **27**, 213 (1982).
- ¹⁹J.-U. Hagenah, G. Meier, G. Fytas, and E. W. Fischer, Polym. J. **19**, 441 (1987).
- ²⁰A. K. Jonscher, Nature **267**, 673 (1977).
- ²¹L. A. Dissado and R. M. Hill, Proc. R. Soc. London, Ser. A **390**, 131 (1983).
- ²²K. L. Ngai and C. T. White, Phys. Rev. B **20**, 2475 (1979).
- ²³Y. Imanishi, K. Adachi, and T. Kotaka, J. Chem. Phys. **89**, 7593 (1988).
- ²⁴W. H. Press, B. O. Flannery, S. A. Teukolsky, and W. T. Vetterling, *Numerical Recipes. The Art of Scientific Computing* (Cambridge University Press, Cambridge, 1986).
- ²⁵P. Hedvig, *Dielectric Spectroscopic of Polymers* (Hilger, Bristol, 1977).
- ²⁶N. G. McCrum, B. E. Read, and G. Williams, *Anelastic and Dielectric Effects in Polymeric Solids* (Wiley, London, 1967).
- ²⁷H. Vogel, Phys. Z. **22**, 645 (1921).
- ²⁸G. S. Fulcher, J. Am. Ceram. Soc. **8**, 339 (1925).